Planar and Homeotropic Alignment of LC Polymers by the Combination of Photoorientation and Self-Organization

Johann Georg Meier,† Ralf Ruhmann, and Joachim Stumpe*

Institute of Thin Film Technology and Microsensoric and Humboldt University Berlin, Department of Chemistry, Erieseering 42, D-10319 Berlin

Received May 26, 1999; Revised Manuscript Received November 18, 1999

ABSTRACT: Upon irradiation with linearly polarized light a photoorientation process occurs in spin-coated films of polymethacrylates with 4-hexyloxyazobenzene side groups containing para methoxy and trifluoromethoxy tail groups. It results in the induction of an oblate orientational distribution perpendicular to the electric field vector causing an optical in-plane anisotropy up to an order parameter of about 0.52. The annealing of the photoreoriented films above T_g results in a prolate homeotropic alignment in the center of the irradiated spot up to a degree of order of 0.78, whereas an amplification of the photoinduced in-plane anisotropy is observed in the interim region to the nonirradiated film area. The development of the in-plane and the out-of-plane components is compared for the photoorientation and the subsequent photoreorientation process in this series of polymers. In both cases, the photogenerated order in the glassy state acts as an initializing force for the thermotropic self-organization resulting in a significant narrowing of an uniaxial orientational distribution. Thus, a photoinduced "command" effect in the bulk of the LC polymers is caused by the combination of both principles of ordering—the photoorientation and the liquid crystallinity.

Introduction

Liquid crystalline polymers with photochromic moieties are promising materials for optical data storage and optical processing.[1−6] Particular interest has been paid to systems containing azobenzene chromophores, thus for instance as command surfaces to align liquid crystals[6,7] or as material for the reversible optical data storage.[1−5] Depending on the material, the supramolecular order of the films and the irradiation conditions different variants have been developed to modify the optical properties by light; such as thermorecording[7,8] photorecording,[9,10] and photoorientation of dispersed azobenzenes in polymer matrixes[11] or of liquid crystalline side group polymers.[12−16] In addition to the well-known photochromism of azobenzenes, the optical properties of photochromic liquid crystalline polymers are changed by the photochemical variation of the supramolecular order. This is caused by the molecular photoisomerization changing not only the electronic structure, but causing in addition a modification of the geometrical shape, the polarity, as well as the direction of the transition moment. The related variation of the degree of order and/or the orientational direction results in a modification of light scattering, dichroism, and birefringence.[1−5]

The photo-(re)orientation process takes place via angular-dependent excitation, a number of angular-selective photoisomerization cycles and rotational diffusion below the glass transition temperature. The repetition of these steps in the steady state of the *E*/*Z* photoisomerization results in an arrangement of the photochromic side groups perpendicular to the electric field vector of the incident light creating an oblate uniaxial orientational distribution.[11−16] The in-plane component of this orientational distribution can be quantified by measuring the angular-dependent absorption of the dichroic dye. The out-of-plane component is accessible by recording the loss of the average absorbance of the in-plane component starting from the isotropic film. It has been demonstrated that the photoorientation of copolymers takes place as a cooperative process whereby the light-induced orientation of the photochromic moieties causes an alignment of the nonphotochromic side groups to the same direction and to a comparable degree of order.[15−25] In this way, an optical axis is generated in films of amorphous polymers[22] or in initially isotropic films of LC polymers[19] or the axis of aligned films of LC polymers[12−17] and LB multilayer systems[25−29] is reoriented.

Very recently, we have shown that the annealing of photooriented films of LC polymers can result in a significant amplification of the optical in-plane anisotropy modifying the photoinduced oblate uniaxial order into a macroscopically uniaxial planar alignment of photochromic LC polymers. In this case the orientational order photogenerated in the glassy state of the polymers acts as an initializing force for the thermotropic self-organization of the LC polymers.[30−33] In analogy to the well-known "command surface" effect, this one represents a photoinduced "command" effect within the bulk. It is caused by the combination of both principles of ordering in one material. This procedure represents a very efficient way to align photochromic LC polymers. It allows the microstructuration of the orientational directions, which is governed exclusively by the electric field vector of the linearly polarized light. Moreover, the procedure results in very high values of optical anisotropy in glassy films of polymers.

The studied azobenzene-functionalized polymethacrylates combine thermotropic liquid crystalline and photochromic properties, whereas the different tail groups (methoxy and trifluoromethoxy) attached to the core introduce a change of the mesophase sequence while

* To whom the correspondence should be addressed.
† Present address: Chalmers University of Technology AB & Göteborg University, School of Physics and Engineering Physics, Department of Microelectronics and Nanoscience, Liquid Crystal Physics, SE-41296 Gothenburg, Sweden.

10.1021/ma990823c CCC: $19.00
Published on Web 01/18/2000

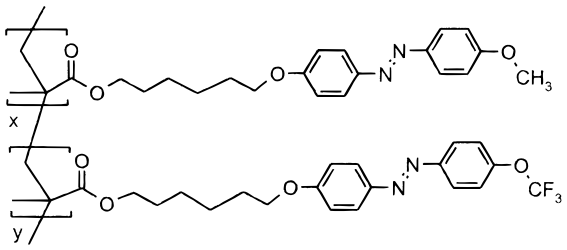

Figure 1. The chemical structure of the polymers.

keeping the molecular dimensions as well as the photophysical properties almost constant.[34,35] In this study the influence of the mesophase on the aligning behavior of photo-(re)oriented films on annealing has been investigated.

Experimental Section

The polymers were synthesized by radical polymerization, which is described elsewhere.[34,35] The molecular weights and the polydispersity indices (M_w/M_n) were obtained from size exclusion chromatography (SEC) using 2PL-gel columns (Knauer) using tetrahydrofuran as eluent and polystyrene as standard. The phase transition temperatures of the polymers were determined by differential scanning calorimetry (DSC) using DSC 7 (Perkin-Elmer). The scanning rate was of 20 K/min. The maxima of the second heating runs were taken as the phase transition temperatures.

Isotropic, transparent films have been prepared by spin-coating using chloroform as solvent. On average, the obtained film-thickness was 0.15 μm. The nonpolarized UV irradiation was performed with a set of a XBO 150 W lamp, water IR filter, and a metal interference filter (365 nm). The power density of the incident light was ~7 mW/cm^2. The samples were irradiated until the steady state has been established. The kinetics of the photoreaction and of the thermal *Z*/*E* isomerization were performed in solution and in films at room temperature using an UV/visible spectrometer Lambda 2 (Perkin-Elmer). The concentration of the solution was 10^{-5} mol/L referred to the repeating unit.

The photo-(re)orientation experiments were performed with the linearly polarized beam of an Ar^+ laser at 457 nm (Innova 90/4 of Coherent). The power density was 20 mW/cm^2. The excitation of the samples with linearly polarized light was carried out in the normal of the film. The angular dependence of the absorbance was measured using a photodiode array UV/visible spectrometer (XDAP, Polytech) in combination with a computer-controlled polarizer with a step-width of 5°. The absorbance at 350 nm was used for the calculation of the dichroic ratio $R = \mathrm{Abs}_{\parallel}/\mathrm{Abs}_{\perp}$. The in-plane order parameter $S = (R - 1)/(R + 2)$ was calculated using R. The out-of-plane order parameter was derived from the average absorbance of the initially isotropic sample and the average absorbance of the homeotropic oriented film to $S_h = 1 - P$ with $P = A_{\mathrm{aligned}}/A_{\mathrm{isotrop}}$. These order parameters have been derived from the order parameter for uniaxial samples of the Maier−Saupe theory. We use these formula to compare the uniaxial liquid crystalline order with the photogenerated order. The in-plane and the out-of-plane order parameters calculated from the projections of the absorbancies on the measuring plane are an approximation if the sample is not uniaxial as it will be discussed for the photoinduced order in the glassy state (spectroscopic order parameter). However, after annealing of the sample a uniaxial order is established. The lateral variation of the anisotropy was checked using a polarizing microscope UV/visible spectrometer (Photo. Mikroskop III Carl Zeiss Oberkochen) with a resolution of 4 μm.

Results and Discussion

Polymer Characterization. The chemical structure of the studied homo- and copolymers is shown in Figure 1. In this series of copolymers, the content of the fluorinated tail group was systematically varied including the two homopolymers. The composition of the polymers was characterized by the determination of the fluorine content.

Table 1. Characteristic Parameters of the Polymer

fluorine value	mole fraction	M_n (10^4 g/mol)	M_w (10^4 g/mol)	M_w/M_n	degree of polymerization
	0	1.9	5.1	2.65	48
1.25	0.10	2.4	6.3	2.67	60
3.79	0.30	1.6	5.6	3.38	39
6.51	0.50	2.2	6.2	2.81	52
6.83	0.54	2.2	5.7	2.61	52
8.73	0.69	2.7	6.7	2.43	62
10	0.79	2.4	5.9	2.46	55
	1	2.3	5.8	2.53	51

Table 2. Phases and Transition Temperatures of the Polymers

mole fraction		phase behavior
PMA 1	0.00	g 75 °C SmA 93.5 °C (ΔH = 744 J/mol) N 134.5 °C (ΔH = 1410 J/mol) I
	0.10	g 72 °C SmA 100.0 °C N 132.0 °C I
	0.30	g 70 °C SmA 120.2 °C N 132.4 °C I
PMA 2	0.50	g 67 °C LC_1 126.5 °C (ΔH = 428 J/mol) LC_2 129.2 °C (ΔH = 3220 J/mol) I
	0.54	g 63 °C LC_1 124.4 °C LC_2 127.0 °C I
	0.69	g 56 °C N 114.0 °C SmA 117.6 °C I
	0.79	g 57 °C N 105.0 °C SmA 112.1 °C I
PMA 3	1.00	g 58 °C N 89.8 °C (ΔH = 559 J/mol) SmA 108.7 °C (ΔH = 1432 J/mol) I

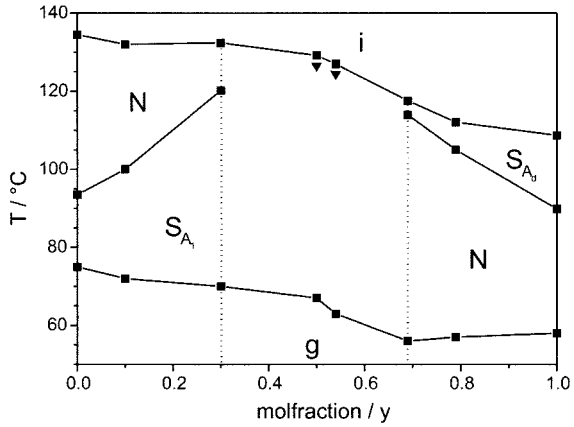

Figure 2. Phase diagram of the polymer series.

The molecular weights were determined by SEC. The variance of the degree of polymerization in these series of polymers is small and can be neglected. The values of uniformity are typical for radical polymerization. Therefore, a significant influence of the differences of the molecular weight on the liquid crystalline properties and the photochemical behavior can be excluded. The results are summarized in Table 1.

The phase transition temperatures and the type of the mesophases of the different polymers were determined by DSC, polarizing microscopy, and small-angle X-ray scattering. The results are summarized in Table 2 and Figure 2. The polymorphism of the series of polymers depends on the proportion of the fluorinated side groups in the polymers. The glass transition temperatures and the clearing temperatures decrease with increasing proportion of the fluorinated tail groups from 75 °C to 58 °C and from 134.5 °C to 108.7 °C, respectively.

In the case of the homopolymer and the copolymers with a distinct excess of the side groups with the

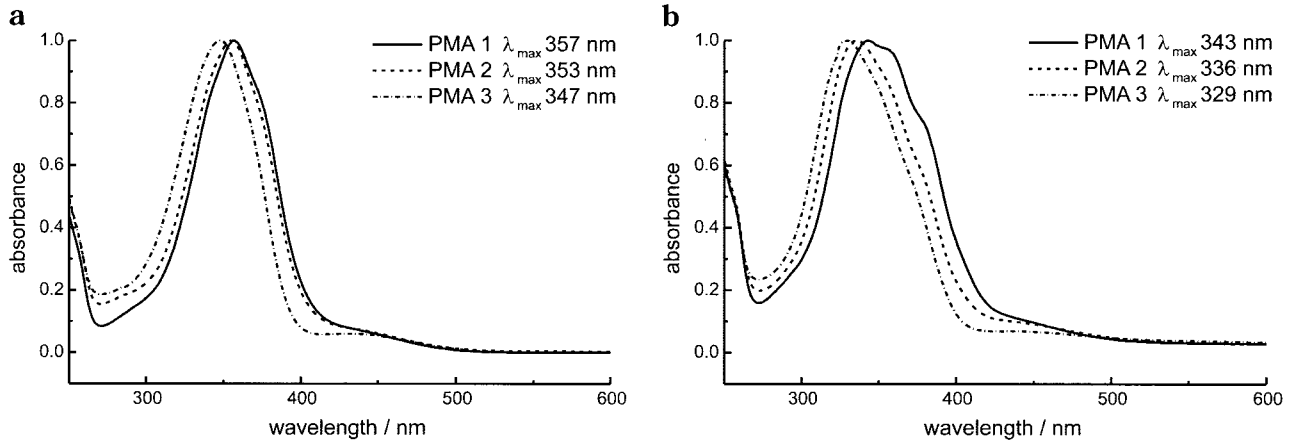

Figure 3. UV/visible spectra of the polymers PMA 1−3 dissolved in chloroform and as spin-coated polymer films.

methoxy tail group, a phase sequence g−SmA−N−I has been found. The homopolymer with the trifluoromethoxy tail group and the copolymers with a clear excess of this substitution show a nematic phase below the SmA phase and a phase sequence g−N−SmA−I has been evident. This nematic phase would have to be referred as reentrant nematic phase if a nematic phase above this SmA phase could have been detected. In the concentration range of 40−60%, referred to the compounds with the trifluoromethoxy tail group, the type of the mesophases could not be determined. The mesophases seem to be characterized by smectic cybotactic preorder in the nematic phase and strong fluctuations of the smectic phase.

The phase transition enthalpy of the LC_1−LC_2 mesophase transition of the one-to-one copolymer is lower than the enthalpies of the equivalent transitions of the homopolymers. It amounts to 428 J/mol for the one-to-one copolymer, 744 J/mol for the nonfluorinated homopolymer and 559 J/mol for the fluorinated homopolymer. The significant change of the liquid crystalline behavior origins from the marginally substitution in the tail group of the mesogene.[34,35]

Spectroscopic Properties and Molecular Photoreaction. The homopolymer with the nonfluorinated tail group (PMA 1), the one-to-one copolymer (PMA 2), and the fluorinated homopolymer (PMA 3) had been selected for further photochemical studies. To characterize the general photochemical behavior, the corresponding azobenzenes as monomeric model compounds and the LC polymers were irradiated in solution using chloroform as solvent. The UV/visible absorption spectra are characterized by a strong, symmetry-allowed $\pi-\pi^*$ transition of the *E* azobenzene moiety at around 350 nm to 360 nm, which is polarized along the molecular long axis and a weak absorption at 450 nm, which originates from the symmetry forbidden $n-\pi^*$ transition. The absorption maxima and the band shapes of the monomeric azobenzenes and of the polymers are identical. Thus, the azobenzene moieties do not interact significantly with each other within the polymer coil in solution.

Comparing the spectra of the polymers in this series the maximum of the $\pi-\pi^*$ band of the *E* isomer is shifted to shorter wavelengths from 357 to 347 nm with increasing proportion of the trifluoromethoxy substitution (Figure 3a). This is caused by the reduction of the electron-donor effect of the para methoxy group by the fluorine atoms in the fluorinated tail group according to the higher electronegativity of the fluorine atoms compared to hydrogen.

Table 3. Absorption Maxima of the Polymers in Dependence of the Molfraction for the Film Samples and in Chloroform

	mol fraction	$\pi-\pi^*$ band (nm)		$\Delta\lambda$ (nm)
		film	solution	solution − film
PMA 1	0	343	357	14
PMA 2	0.5	336	353	17
PMA 3	1	329	347	18

Spin-coating of solutions of these liquid crystalline polymers results in transparent, isotropic films. The $\pi-\pi^*$ transition is hypsochromically shifted and the shape of the band becomes asymmetric compared to the spectra in solution. In contrast to that, the local $n-\pi^*$ transition remained unchanged. The asymmetry of the $\pi-\pi^*$ band can be related to molecular aggregation of the azobenzene moieties.[26] Thus, in addition to intermolecular interaction causing liquid crystallinity the strong dipole−dipole interactions of the aromatic side groups result in the formation of dimers or higher aggregates by π-stacking on local scale. In contrast to the solution, the (*E*)-azobenzene moieties are not independent from each other in the films. As already observed in solution an increase of the hypsochromic shift of the absorption is found in dependence on the proportion of the fluorinated tail group in the polymers (Figure 3b). In addition the tendency of aggregation increases with a larger proportion of the trifluoromethoxy groups (Table 3).

Upon irradiation, the azobenzene moieties undergo *E*/*Z* photoisomerization and a wavelength-dependent steady state between the thermodynamically stable rodlike *E* and the metastable, crooked *Z* isomer is established. The transition moment of the $\pi-\pi^*$ band of the *Z* isomer is directed along the N=N double bond. Compared to the *E* isomer the $\pi-\pi^*$ transition of the *Z* isomer is shifted to shorter wavelengths and its absorption is decreased. In contrast to the *E* isomer the $n-\pi^*$ transition is symmetry-allowed in the *Z* conformation. Therefore, the absorption of the $n-\pi^*$ band is increased by the photoisomerization. Thermal *Z*/*E* isomerization rebuilds the *E* isomeric form in the darkness.

The steady state of the photoisomerization is determined by the inverse ratio of the extinction coefficients of the *E* and *Z* isomer at the excitation wavelength. Thus, UV irradiation (365 nm) generates a steady state with a high amount of *Z* isomers and the visible

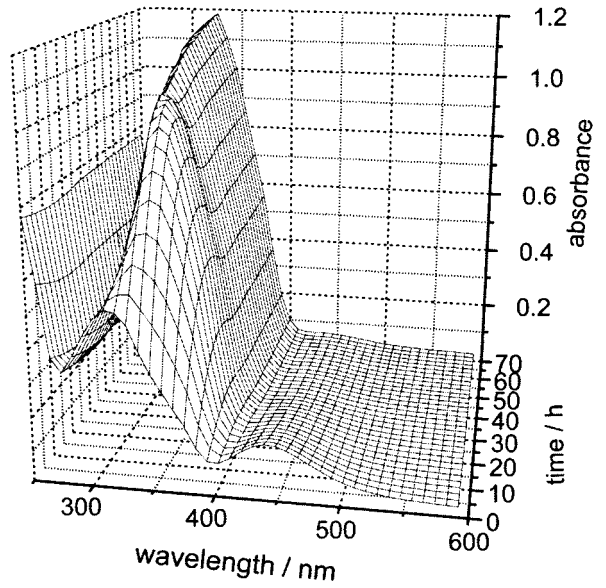

Figure 4. Change of UV/visible spectra caused by thermal *Z*/*E* isomerization after UV irradiation of a PMA **3** film.

irradiation (457 nm) generates an *E* isomer rich state in the case of these azobenzenes. The spectroscopic course of the photoisomerization in solution shows isosbestic points for the homopolymers, indicating uniform photoreactions. However, the copolymers consisting of two differently substituted azobenzenes did not show isosbestic points. The subsequent thermal *Z*/*E* isomerization rebuilt the initial state completely, demonstrating the reversibility of the reaction. The absorbance−time diagrams of the thermal *Z*/*E* isomerization were fitted well by the monoexponential function $f(t) = A + B(1 - e^{-kt})$ using the $\pi-\pi^*$ band at 350 nm. The rate constant of the thermal isomerization is significantly slower for the trifluoromethoxyazobenzene compared to the nonfluorinated monomer as well as the related polymer. The rate constants, *k*, were determined to be 1.202 h^{-1} for PMA 1 and 0.057 h^{-1} for PMA 3 in chloroform at room temperature. The constants of the monomeric 4-methoxy-4′-alkoxyazobenzene amounted to about 0.159 and 0.036 h^{-1} for the fluorinated one. The difference should be caused by the different polarity and mobility in the dissolved polymeric coil compared to the related monomers in the polar solvent.

In contrast to the behavior of the homopolymers in solution, no isosbestic points are observed for the photoisomerization in films. Because there is no doubt about the uniformity of the photoisomerization itself, it indicates that the molecular photoreaction generates additional changes in the supramolecular order. Even a small amount of *Z* isomers results in the distortion of the aggregates, causing an increase of absorbance (Figure 4). This spectral behavior in the spin-coated LCP films is similar to aggregated azobenzene moieties in LB multilayers on irradiation.[26] The process is thermally reversible in the films too. The trifluoromethoxy-substituted group isomerizes slower ($k = 0.063$ h^{-1}) than the nonfluorinated species ($k = 0.309$ h^{-1}), as already observed for the reaction in solution. Surprisingly, the absorption maxima of the samples PMA 1 and PMA 2 have shifted 3 nm to longer wavelengths compared with the initial state. PMA 3 did not show this shift (Table 4), indicating the stronger aggregation tendency. Pursuing the thermal *Z*/*E* isomerization in darkness, a shift of the maximum of the developing $\pi-\pi^*$ band under

Table 4. Absorption Maxima of the Film Samples before and after the Isomerization Cycle

	absorption maxima (nm)	
	initial state	after thermal isomerization
PMA 1	343	346
PMA 2	336	339
PMA 3	329	329

further growing has been observed (Figure 4). In the case of PMA 3 the band starts to evolve at around 340 nm followed by a hypsochromic shift of the absorption maximum of ∼10 nm reaching the initial state. The maximum at 340 nm in the initial part corresponds to nonaggregated monomer, but establishing a high amount of rodlike *E* isomers the aggregation process starts and causes the shift of the $\pi-\pi^*$ maximum to 330 nm. The other samples exhibit generally the same behavior but do not reaggregate to the full extent caused by the lower mobility due to the higher T_g's.

Photoorientation. Transparent isotropic films are prepared by spin-coating. The azobenzene side groups of the LC polymers are aggregated due to the properties of the material. The irradiation of such films with linearly polarized light (457 nm) generates low values of optical anisotropy, which are not reproducible caused by the aggregation. Therefore, different polymers cannot be compared. For this reason, an initial UV irradiation step (365 nm, 7 mW/cm^2) is carried out before the linearly polarized visible exposure. The established steady state with a high amount of the *Z* isomeric form causes the destruction of the H aggregates.[26] This procedure creates a common starting state and eliminates the dissimilar extensions of the aggregation of the different polymers and samples. The states after the photochemical pretreatment are comparable for all three polymers of this series. Thus, the procedure results in films with random distribution of the side groups, which are nonaggregated, and do not show any supramolecular order. Subsequent linearly visible irradiation immediately establishes a steady state with a high amount of *E* isomers, which exist initially as isolated, nonaggregated chromophores. Certainly, the micromorphology and the dynamics are changed by this photochemical pretreatment, transferring the system photochemically in a more mobile, nonequilibrium state.

Optical anisotropy is generated by photoorientation processes in the glassy state of the polymers. On continued irradiation with linearly polarized light (457 nm, 20 mW/cm^2), the photochromic side groups become oriented perpendicular to the electric field vector establishing an oblate uniaxial order. To quantify the in-plane component of this order the spectroscopic order parameter has been calculated using the dichroic ratio at the absorbance maximum at about 350 nm.

In Figure 5 the evolution of the in-plane order parameter and the average absorbances of the samples are compared for the photoorientation and the photoreorientation process of these three polymers. A photoreorientation process is caused by the change of the electric field vector of the incident light with respect to the sample.

At the beginning of the polarized visible exposure the average absorbance increases very fast, establishing the new steady state of the 4,4′-dialkoxyazobenzene side groups related to the exposure with monochromatic light of wavelength 457 nm. The molecular photoprocess is

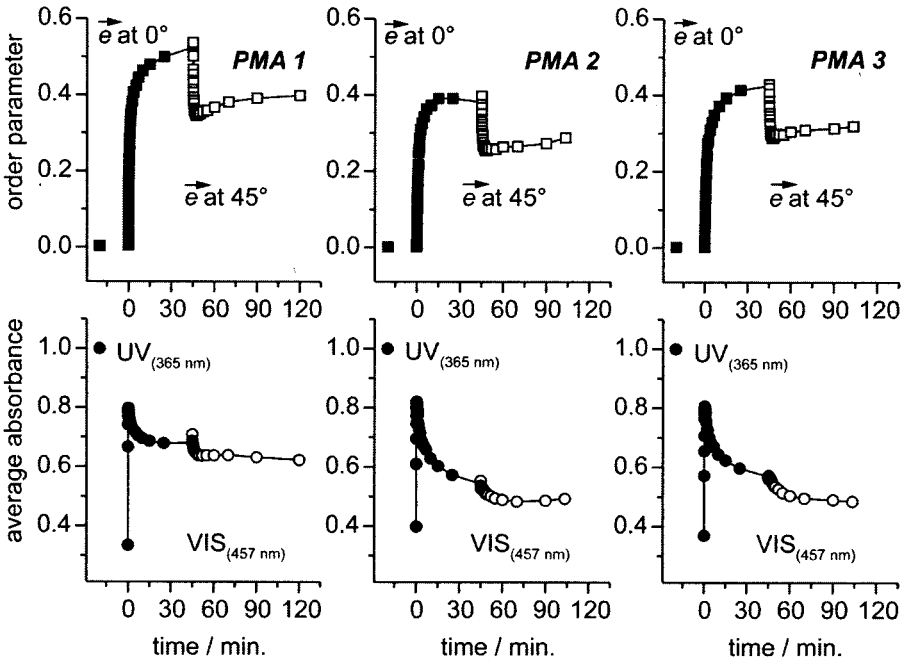

Figure 5. The evolution of spectroscopic order parameter, *S*, and average absorbance measured at 350 nm during the photoorientation and the subsequent photoreorientation process changing the azimuth angle of the electric field vector by 45°.

finished in about 14 s in the case of all three polymers. A dynamic equilibrium is established, which is characterized by a content of 10−20% of *Z* isomers and simultaneously the orientation process is going on. Within this time, the order parameter has only developed up to 0.15 for PMA 1, 0.09 for PMA 2, and 0.06 for PMA 3, demonstrating that the main part of the orientation process takes place in the steady state of the photoisomerization. Figure 5 shows that there exist well-developed maxima of the average absorbance in all samples. The further irradiation causes a decrease of absorbance during the orientation process. This is caused by an increasing proportion of the azobenzene moieties that becomes oriented in direction of the light propagation. In this way, an oblate orientational plane is populated perpendicular to the electric field vector of the incident light characterized by an in-plane and an out-of-plane component. The normalized difference of the absorbance between the steady state and the finally photooriented sample is 0.12 for PMA 1, 0.28 for PMA 2, and 0.24 for PMA 3. It shows that the decrease is much larger for the fluorine containing polymers then for the nonfluorinated sample indicating that the fluorinated samples have a stronger tendency for establishing a homeotropic alignment. The reason for the different behaviors of the polymers in this series is not clear so far. It could be caused by the different mesophases, different mobilities, or differences in the interfacial properties modified by the fluorinated tail groups.

Upon continued irradiation, the saturation values of the optical anisotropy are established. The final in-plane order parameter was found to 0.52 for PMA 1 and for the fluorine-containing polymers PMA 2 and PMA 3 to 0.40 and 0.42 performing the orientation process under identical irradiation conditions. The value of PMA 1 is significantly higher compared with the other ones. This polymer is characterized by a higher glass transition temperature of about 17 °C compared to PMA 3 and the highest phase transition enthalpy SmA/N within the series. As shown for other LC polymers[24] too, the maximum of optical anisotropy generated in the glassy state seems to correspond to the phase transition enthalpies or the liquid crystalline ordering tendency of the polymers, respectively.

Table 5. In-Plane (*S*) and Out-of-Plane Component (S_h) of the Orientational Distribution and Average Absorbance in the Photooriented, the Thermally Relaxed Photooriented, and the Photoreoriented States for PMA 1−3

	photooriented	thermally relaxed	photoreoriented
		in-plane order (*S*)	
PMA 1	0.52	0.54	0.40
PMA 2	0.38	0.40	0.29
PMA 3	0.42	0.43	0.32
		out-of-plane order (S_h)	
PMA 1	0.32	0.29	0.38
PMA 2	0.46	0.45	0.51
PMA 3	0.43	0.44	0.52
		average absorbance	
PMA 1	0.68	0.71	0.62
PMA 2	0.54	0.55	0.49
PMA 3	0.57	0.56	0.48

Thermal *Z*/*E* isomerization of the 10−20% Z isomers, existing during the photoorientation process, and structural relaxation takes place on storage in darkness. In this way, the average absorbance is slightly increased in the case of PMA 1 and 2, but it is decreased slightly in PMA 3. Simultaneously, the in-plane order is increased slightly in all polymer films decreasing the out-of-plane component in PMA 1 and 2 (Table 5). These observations indicate as well that the fluorinated polymer PMA 3 has a stronger tendency for a homeotropic alignment, while in the case of PMA 1 a small amplification of the in-plane order occurs.

Photoreorientation. Turning the sample 45° with respect to the polarization plane of the incident light a new criterion is given for the angular-dependent photoselection and the subsequent photoorientation process. The photoreorientation experiment ($\vec{e}$ at 45°) was carried out starting from thermally relaxed photooriented samples. An azimuth angle of 45° was chosen between the photoinduced optical axis and the electric field vector

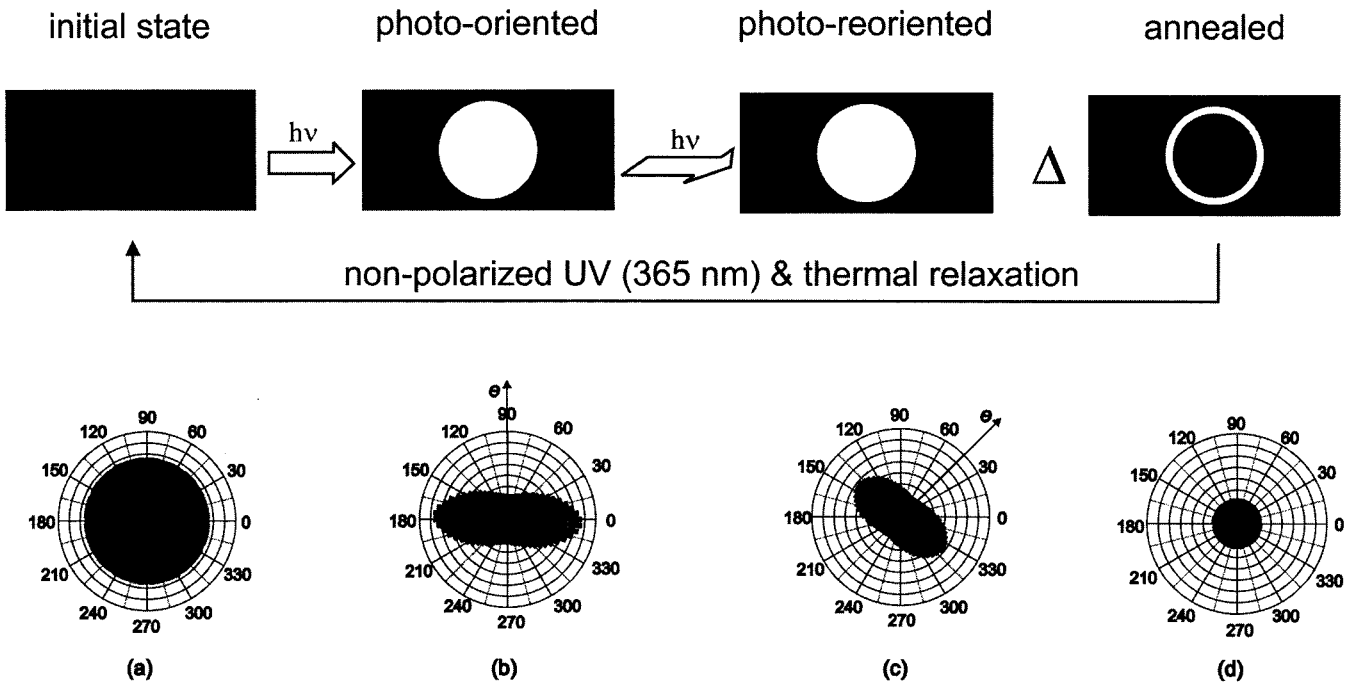

Figure 6. Schemes of the polarized microscope pictures between crossed polarizers and the related angular-dependent absorbance of these steps.

of the second irradiation step. *Z* isomers are generated again corresponding to the steady state at 457 nm, decreasing the absorbance. A significant decrease of the in-plane order is observed in the beginning of the photoreorientation (Figure 5). After 180 s, a minimum of the degree of order of about 0.3 is found for all three polymers. This minimum is not only related to the establishment of the steady state, which is reached within a few seconds, but the photoreorientation decreases the initially photoinduced order, generating a new one which corresponds to the new photoselection criterion. Thus, on continued irradiation the optical axis is turned continuously from the initial position at 45° with respect to $\vec{e}$ toward the final angle of 90°. As shown recently the photoreorientation of oriented samples of LC polymers is less efficient than the photoorientation of isotropic films[23] because the initial order has to be overcome. The azobenzene side groups become reoriented perpendicular with respect to the new direction of polarization. During this process the orientational order increases slightly establishing the new direction and new saturation values. An in-plane degree of order is found to be about 0.4 for PMA 1 and only 0.29 and 0.32 for PMA 2 and PMA 3. Compared to the final states of the photoorientation process both the degree of order and the average absorbance are significantly smaller in the photoreoriented films. However, the out-of-plane order shows an opposite development (Table 5). The incident light cannot excite the azobenzene moieties aligned in the propagation direction of the laser light, because their excitation probability is zero.

The interaction with azobenzene moieties which have an in-plane component results in the generation of a new orientational distribution perpendicular to $\vec{e}$. Compared to the final state of the photoorientation process, the out-of-plane component is increased as a consequence of the second photoorientation process. This results in an additional part of the chromophores which becomes aligned in the propagation direction. Compared to the normalized absorbance of the initial isotropic films of 1.0, the average absorbance is 0.62 for PMA 1 and is more strongly decreased in the cases of PMA 2 and PMA 3, which are found to 0.49 and 0.48.

Annealing. Annealing of the samples into the first mesophase develops the photoinduced oblate uniaxial order into a prolate uniaxial order.[30−32] The influence of these different mesophases may reveal the nature of this self-ordering process.

Figure 6 shows the history of the photoreoriented sample which is annealed 15 °C above the glass transition temperature for 60 min. Visualizing the birefringence and the anisotropic spectral properties of the specimen, the scheme illustrates the different steps of the procedure characterized by microscopical observation between crossed polarizers and by the corresponding angular-dependent absorption at 350 nm.

Starting from the isotropic film (Figure 6a) an optical axis has been developed perpendicular to the $\vec{e}$ vector of the incident light in the irradiated area (Figure 6b). The microscopic observation shows the irradiated and in this way oriented area of the laser spot as bright, birefringent circle surrounded by the dark, nonbirefringent isotropic film. Rotating the sample, the optical axis can be detected. The polar diagram shows the corresponding in-plane component of the orientational distribution of the azobenzene side groups measured over the entire irradiated area. The results of the reorientation process are shown in Figure 6c, whereas the crossed polarizers were turned compared to Figure 6b to obtain maximum contrast. The annealing above the glass transition temperature results in a bright birefringent ring at the border region of the irradiated spot to the nonirradiated area and in a dark, nonbirefringent center (Figure 6d). The polar diagram shows that the in-plane anisotropy is erased in the center. It becomes optically isotropic. Moreover, the average absorbance of the center is significantly decreased comparing this area of Figure 6d and of Figure 6c. The scheme also illustrates that the average absorbance decreases from one step to the next one indicating the increase of the out-of-

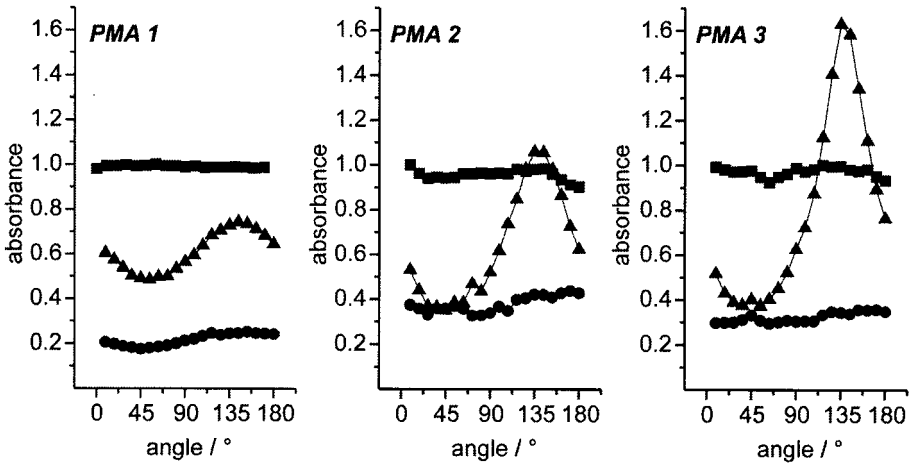

Figure 7. The angular-dependent absorbance measured in the $\pi-\pi^*$ band of the azobenzene moiety (350 nm) at the different areas of the sample as shown in Figure 8d: (■) nonirradiated area, (▲) birefringent ring, and (●) center of the irradiated spot.

Table 6. Spectroscopic Order Parameter and Average Absorbance in the Different Areas of the Annealed Samples of PMA 1−3 (Data Obtained from Figure 7)

	center		birefringent ring		nonirradiated region	
compound	S_h	A	S	A	S	A
PMA 1	0.781	0.217	0.152	0.608	0.007	0.990
PMA 2	0.604	0.379	0.402	0.637	0.034	0.957
PMA 3	0.668	0.323	0.529	0.796	0.026	0.972

plane component of the absorbance of the rodlike (*E*)-azobenzene side groups.

A more detailed insight was obtained by detecting the local absorbance and its orientational distribution of the different areas in the samples using a polarization microscope UV/visible spectrometer (Figure 7). After annealing, the center of the spot no longer exhibits in-plane anisotropy, and the average absorbance of all polymers is dramatically decreased. The out-of-plane order parameter S_h was calculated from the average absorbance of the initial isotropic and the aligned film, which amounts to 0.78 for PMA 1, 0.60 for PMA 2, and 0.67 for PMA 3 (Table 6). The established degree of order corresponds with the enthalpy of the mesophase transition LC_1 to LC_2. The direction of the anisotropy within the ring is the same as in the photoreoriented film. Depending on the polymer the degree of order decreased from 0.4 to 0.15 in the case of polymer PMA 1, the polymer with a SmA−N mesophase sequence, but it is amplified for PMA 3 the polymer with a phase sequence N−SmA from 0.32 to 0.5, while the nonirradiated areas of all 3 polymers were not significantly affected.

All these facts together demonstrate that the photochromic side groups of the LC polymers become homeotropically aligned in the center of the photoreoriented film and planar aligned at the transition to the nonirradiated area by annealing. The result is very surprising insofar that it was expected to generate either a planar or a homeotropic order but not both types of orientation.

The degrees of order of the homeotropic centers correspond with the tendency of phase transition enthalpies of the polymers. The type of the underlying mesophase seems to have no significant influence. Within the ring structure an amplification of in-plane anisotropy takes place for the fluorine-containing polymers. The increasing in-plane order with higher content of the fluoro-substituted tail group might be attributed to the change in the underlying mesophase from SmA for PMA 1 to N for PMA 3. The preference of smectic materials to undergo homeotropic orientation is a well-known fact. Nevertheless, the development of the both types of orientation on annealing in a monodomain-like prealigned liquid crystalline material is not completely understood so far, but it is most probably related to that this transition region was exposed with lower power density due to the intensity profile of the laser beam generating a different orientational order compared to the center.

The combination of UV irradiation and following thermal isomerization results in an isotropic film which has an absorbance that is comparable to the initial film. In this way, any anisotropy is erased photochemically. This demonstrates that there is not any photodegradation. All effects are exclusively caused by photoorientation or photostimulated alignment. Moreover, it demonstrates the reversibility of all changes.

Conclusion

The photoorientation process in the glassy state of the photochromic polymers results in the orientation of the azobenzene moieties generating an oblate orientational plane perpendicular to the electric field vector. The in-plane component is visualized by the dichroism and birefringence, whereas the measuring beam agrees with the film normal. The significant decrease of absorbance indicates the increasing orientation of azobenzenes in the direction of the light propagation. As shown, this out-of-plane component of the orientational distribution is increased as a consequence of the multistep photoorientation process by changing the azimuthal angle between the sample and the electric field vector. Comparing the studied polymers PMA 1−3 only slight differences in the efficiency and the values of photoinduced dichroism for the photoorientation and the photoreorientation process in the glassy state have been detected, which are graded with the phase transition enthalpies of the mesophase.

The interaction of the ordering impact of the polarized light and thermotropic self-organization of LC polymers is of exceptional interest.[30−33] Annealing modifies the order of the photoreoriented samples dramatically. Thus, in this series the annealing above T_g within the mesophases causes a locally different development of the photogenerated oblate uniaxial alignment of the LC polymers. Starting from the differently developed photoinduced order, either excess of the in-plane or the out-

of-plane component, the thermotropic self-organization of the LC polymer results alternatively in a planar or a homeotropic alignment. The annealed films of polymers PMA 1−3, irradiated to the saturation values of the second photoreorientation step, develop a homeotropic alignment up to degree of order of about 0.78 in the spot surrounded by an in-plane anisotropic ring structure located in the less photooriented transition region to the isotropic nonirradiated film. The in-plane anisotropy is amplified in the case of PMA 3, the polymer with the underlying nematic phase, and it is reduced in the case of PMA 1, the polymer with the underlying SmA phase. The alignment seems to depend on the polymer structure, especially from the resulting mesophase properties such as phase type and transition enthalpy, the interfacial interactions, and the photoinduced order.

The result is surprising because, recently, a significant amplification of the in-plane anisotropy was reported for similar liquid crystalline side group copolymers.[30,31] Thus, a planar alignment to a degree of order up to 0.8 was developed in the case of some smectic copolymethacrylates under comparable conditions. In both cases the orientational order photogenerated in the glassy state acts as an initializing force for the thermotropic self-organization process resulting in a significant narrowing of the orientational distribution. The results indicate that the final order depends very sensitively on the primary photoinduced order. In some cases the in-plane component and in other cases the out-of-plane component of the photoinduced oblate order dominates the following aligning process resulting in planar or homeotropic liquid crystalline monodomains. It represents a photoinduced "command" effect in the bulk of LC polymers in analogy to the well-known "command surface" effect of liquid crystals on photoinduced anisotropic surfaces. The effect is caused by the combination of both ordering principles—photoorientation and liquid crystallinity in one material. It offers a new way to align photochromic LC polymers by light.

References and Notes

(1) McArdle, C. B. In *Side chain liquid crystalline Polymers*; McArdle, C. B., Ed.; Blackie: London, 1989.
(2) Xie, S.; Natansohn, A.; Rochon, P. *Chem. Mater* **1993**, *5*, 403.
(3) Shibaev, V. P.; Kostromin, S. G.; Ivanov, S. A. In *Polymers as Electrooptical and Photooptical Active Media*; Shibaev, V. P., Ed.; Springer: New York, 1996.
(4) Fuhrmann, T.; Wendorff, J. In *Polymer Liquid Crystals*; Brostow, W., Collyer, A., Eds.; Chapman and Hall: New York, 1997; Vol. 4.
(5) Ichimura, K.; Seki, T.; Kawanishi, Y.; Y. Suzuki, M. S.; Tamaki, T. In *Photoreactive Materials for Ultrahigh-Density Optical Memories*, Irie, M., Ed.; Elsevier: Amsterdam, 1994.
(6) Ichimura, K. In *Polymers as Electrooptical and Photooptical Active Media*, Shibaev, V., Ed.; Springer: New York, 1996.
(7) Plate, N. A.; Talroze, R. V.; Shibaev, V. P. *Appl. Chem.* **1984**, *56*, 403.
(8) Coles, H. J.; Simon, R. *Polymer* **1985**, *26*, 1801.
(9) Ikeda, T.; Horiuchi, S.; Karanjit, D. B.; Kurihara, S.; Tazuke, S. *Macromolecules* **1990**, *23*, 36.
(10) Ikeda, T.; Horiuchi, S.; Karanjit, D. B.; Kurihara, S.; Tazuke, S. *Macromolecules* **1990**, *23*, 42.
(11) Todorov, T.; Nikolova, L.; Tomova, N. *Appl. Opt.* **1984**, *23*, 4309.
(12) Eich, M.; Wendorff, J. H.; Reck, B.; Ringsdorf, H. *Makromol. Chem., Rapid. Commun.* **1987**, *8*, 59.
(13) Eich, M.; Wendorff, J. H. *Makromol. Chem., Rapid. Commun.* **1987**, *8*, 467.
(14) Shibaev, V.; Yakovlev, I.; Kostromin, S.; Ivanov, S.; Zverkova, T. *Vysokomol. Soed.* **1990**, *A32*, 1552.
(15) Stumpe, J.; Müller, L.; Kreysig, D.; Hauck, G.; Koswig, H. D.; Ruhmann, R.; Rübner, J. *Makromol. Chem., Rapid Commun.* **1991**, *12*, 81.
(16) Ivanov, S.; Yakovlev, I.; Kostromin, S.; Shibaev, V.; Läsker, L.; Stumpe, J.; Kreysig, D. *Makromol. Chem., Rapid Commun.* **1991**, *12*, 709.
(17) Stumpe, J.; Läsker, L.; Fischer, T.; Kostromin, S. *J. Photochem. Photobiol., A: Chem* **1994**, *80*, 453.
(18) Läsker, L.; Stumpe, J.; Fischer, T.; Kostromin, S.; Ivanov, S.; Shibaev, V.; Ruhmann, R. *Mol. Cryst. Liq. Cryst.* **1994**, *253*, 1.
(19) Läsker, L.; Stumpe, J.; Fischer, T.; Kostromin, S.; Ivanov, S.; Shibaev, V.; Ruhmann, R. *Mol. Cryst. Liq. Cryst.* **1994**, *253*, 293.
(20) Menzel, H.; Rüther, M.; Stumpe, J.; Fischer, T. *Supramol. Sci*, **1998**, *5*, 1−2, 49.
(21) Fischer, T.; Menzel, H.; Stumpe, J. *Supramol. Sci.* **1997**, *4*, 3−4, 543.
(22) Läsker, L.; Fischer, T.; Stumpe, J.; Kostromin, S.; Ivanov, S.; Shibaev, V.; Ruhmann, R. *Mol. Cryst. Liq. Cryst.* **1994**, *246*, 347.
(23) Stumpe, J.; Läsker, L.; Fischer, T.; Rutloh, M.; Kostromin, S.; Ruhmann, R. *Mol. Cryst. Liq. Cryst.* **1995**, *261*, 371.
(24) Stumpe, J.; Läsker, L.; Fischer, T.; Kostromin, S.; Ruhmann, R. *Thin Solid Films* **1996**, *285*, 252.
(25) Barnik, M. I.; Kozenkov, V. M.; Shytykov, N. M.; Palto, S. P.; Yudin, S. G. *J. Mol. Electron.* **1989**, *5*, 53.
(26) Geue, T.; Ziegler, A.; Stumpe, J. *Macromolecules* **1997**, *30*, 5729.
(27) Geue, T.; Stumpe, J.; Pietsch, U.; Haak, M.; Kaupp, G. *Mol. Cryst. Liq. Cryst.* **1995**, *262*, 157.
(28) Geue, T.; Stumpe, J.; Möbius, G.; Pietsch, U.; A. Schuster; Ringsdorf, H. *Mol. Cryst. Liq. Cryst.* **1994**, *246*, 405.
(29) Stumpe, J.; Geue, T.; Fischer, T.; Menzel, H. *Thin Solid Films* **1996**, *285*, 606.
(30) Fischer, T.; Läsker, L.; Czapla, S.; Rübner, J.; Stumpe, J. *Mol. Cryst. Liq. Cryst.* **1997**, *297*, 498.
(31) Fischer, T.; Läsker, L.; Rutloh, M.; Czapla, S.; Stumpe, J. *Mol. Cryst. Liq. Cryst.* **1997**, *299*, 293.
(32) Stumpe, J.; Fischer, T.; Czapla, S. *Macromol. Chem. Phys., Macromol. Symp.* **1998**.
(33) Stumpe, J.; Fischer, T.; Rutloh, M.; Meier, J. G. *Polym. Prepr.* **1998**, *39*, 308.
(34) Prescher, D.; Thiele, T.; Ruhmann, R.; Schulz, G. *J. Fluorine Chem.* **1995**, *74*, 185.
(35) Ruhmann, R.; Thiele, T.; Prescher, D.; Wolff, D. *Macromol. Rapid Commun.* **1995**, *16*, 161.

MA990823C